TRANSACTIONS OF THE INSTITUTE OF MEASUREMENT & CONTROL

Article

Transactions of the Institute of Measurement and Control
2019, Vol. 41(11) 3033–3042

DOI: 10.1177/0142331218819705
journals.sagepub.com/home/tim
SAGE

State tracking control of nonlinear systems using neural adaptive dynamic sliding mode

Ali Karami-Mollaee[1], Hamed Tirandaz[1] and Oscar Barambones[2]

Abstract

This paper describes control issues of a general-class, single-input, unknown, nonlinear, non-affine system using dynamic sliding-mode control (DSMC). Chattering can be removed in DSMC with an integrator as a low-pass filter, placed before the input control signal of the plant. As a result, the augmented system (which contains the integrator) in DSMC has one more dimension than the actual system. Then the plant model must be completely known. To overcome this problem and to identify the plant model, an adaptive radial basis-function neural network has been employed and a robust procedure developed to train the parameters of a neural network based on Lyapunov theory. A smooth controller has been developed and some numerical simulations have been performed to verify the validity of the proposed approach. Two nonlinear systems were used for simulation: a Duffing–Holmes chaotic system and a switch reluctance motor. The advantage of the presented approach is that the system model can be considered unknown and can be in non-affine form.

Keywords

Neural network, dynamic sliding-mode control, chattering, chaotic system, switch reluctance motor

Introduction

In the literature, sliding-mode control has been utilized as a powerful technique because of its invariance property in facing matched structured or unstructured uncertainties and disturbances that cause challenges in the realization of any proposed control law for real systems (Perruquetti and Barbot, 2002; Slotine and Li, 1991; Young et al., 1996). Invariance means insensitivity to parameter variations (Moghaddam et al., 2011) and is somewhat stronger than robustness (Perruquetti and Barbot, 2002). Chattering is the greatest disadvantage of sliding-mode control (Boiko et al., 2005; Lee and Utkin, 2007).

To solve this problem and remove chattering, five methodologies have been proposed. These are the boundary layer (Slotine and Li, 1991; Young et al., 1996), the adaptive boundary layer (Perruquetti and Barbot, 2002; Slotine and Li, 1991; Young et al., 1996), higher-order sliding-mode control (Bartolini et al., 1998; Levant, 1993, 2003, 2005), dynamic sliding-mode control (DSMC) (Chen et al., 2007; Karami-Mollaee et al., 2011) and an intelligent approach (Kaynak et al., 2001). The invariance property of slidingmode control could not be preserved in the boundary layer and adaptive boundary layer approaches (Chen et al., 2002). Higher-order sliding-mode control is proposed to reliably prevent chattering (Cavallo and Natale, 2003; Laghrouche et al., 2007). In higher-order sliding-mode control, the effect of switching can be completely removed by moving the switching task to the higher-order derivatives of the desired output (Moghaddam et al., 2011). Many algorithms have been proposed for the implementation of second- or higher-order sliding-mode control (Bartolini et al., 1998). However, calculation of the higher-order derivative of the plant model is the main drawback of these designed control laws (Bartolini et al., 1998; Cavallo and Natale, 2003; Laghrouche et al., 2007; Levant, 1993, 2003, 2005). It is well-known that when the relative degree is two, the plant model derivative must usually be known using some observers, for instance the sliding differentiator utilized by Levant (1998). In DSMC, an integrator (or any other strictly low-pass filter) would be inserted before the input control signal of the plant. In this way, switching would be removed from the input control signal, since the integrator filters the high frequencies, owing to the use of the signum function in sliding-mode control (Slotine and Li, 1991). However, to control the augmented system in DSMC, the plant model must be completely known, because the augmented system has one more dimension than the actual system (Karami-Mollaee et al., 2011). Therefore, in DSMC, the plant model is needed but in higher-order sliding-mode control the derivatives of the plant model must be known; this is the

[1]Electrical and Computer Engineering Faculty, Hakim Sabzevari University, Iran
[2]Automatic Control and System Engineering Department, University of the Basque Country, Spain

Corresponding author:
Ali Karami-Mollaee, Electrical and Computer Engineering Faculty, Hakim Sabzevari University, Sabzevar, Iran.
Email: karami@hsu.ac.ir

main advantage of the DSMC approach, compared with the higher-order sliding-mode control approach. For example, Chen et al. (2007) proposed a two-dimensional loop transfer recovery observer to estimate the uncertainty in the DSMC. In this work, Chen et al. (2007) assumed that the disturbance and its derivative were bounded, but this limited their work. To overcome this problem, Karami-Mollaee et al. (2011) introduced a new method based on DSMC using neural networks, based on the definition of a complicated sliding surface.

More recently, considerable effort has been made to solve the problem of chattering in sliding-mode control using an intelligent approach (Amer et al., 2011; Bouzeriba et al., 2016; Hao et al., 2016; Kaynak et al., 2001; Sun et al., 2011; Wu et al., 2017; Xu et al., 2016; Yang and Yan, 2016; Yildiz et al., 2007). Most of these methods are devoted to affine systems (Erbatur and Kaynak, 2001; Levant, 2005; Wong et al., 2001). The intelligent methods can be placed into two categories: direct methods and indirect methods (Norgaard et al., 2000). In direct methods, these approaches are applied to the controller itself; in indirect methods, these approaches play a secondary role in the controller (Norgaard et al., 2000).

We propose the use of an adaptive-neural-network observer to solve the estimation problem of the sliding surface in DSMC. The unknown part of the sliding surface can be estimated using this observer. As a result, the sliding surface would be available. Thus, the proposed adaptive-neural-network observer is an indirect approach. The structure of the proposed observer is based on a radial basis-function neural network (RBFN). We have proposed online estimation parameters based on the RBFN to guarantee the robustness of our proposed method. The stability analysis and the validity of convergence of the proposed neural model and the controller are demonstrated using Lyapunov functions. The use of both sliding-mode and adaptive techniques make the developed control law more robust and powerful for the control of non-affine uncertain systems. Thus, the proposed neural network observer is in the indirect category.

The remainder of this paper is organized as follows. The next section provides some preliminary details and gives the background for the work and the problem formulation. After this, an adaptive-neural-network observer is presented to overcome the problem of DSMC and the design of the control variable using the sliding surface is described. Then some numerical simulations are illustrated, to verify theoretical concepts presented in the previous sections. Finally, some concluding remarks are made. Some proofs are given in an appendix.

Plant and controller formulation

Consider a global structure of nonlinear non-affine system with state-space representation, as

$$\begin{aligned} \dot{z}_i &= z_{i+1}, \qquad i = 1, 2, \ldots, n-1 \\ \dot{z}_n &= f(z, u) \\ z &= [z_1, z_2, z_3, \cdots, z_n]^{\mathrm{T}} \end{aligned} \tag{1}$$

where $z(t) \in R^n$ denotes the accessible state vector of the non-affine system, $u(t) \in R$ represents the control input of the system and $f(z(t), u(t)) : R^{n+1} \rightarrow R$ represents an unknown nonlinear function. The other form of this equation is

$$\dot{z} = Az + Bg(z, u) \tag{2}$$

such that

$$g(z, u) = f(z, u) + \sum_{i=1}^{n} a_{n-i+1} z_i \tag{3}$$

and

$$A = \begin{bmatrix} 0 & 1 & 0 & \cdots & 0 \\ 0 & 0 & 1 & \ddots & \vdots \\ \vdots & \vdots & \ddots & \ddots & 0 \\ 0 & 0 & \cdots & 0 & 1 \\ -a_n & -a_{n-1} & \cdots & -a_2 & -a_1 \end{bmatrix}, \quad B = \begin{bmatrix} 0 \\ 0 \\ \vdots \\ 0 \\ 1 \end{bmatrix} \tag{4}$$

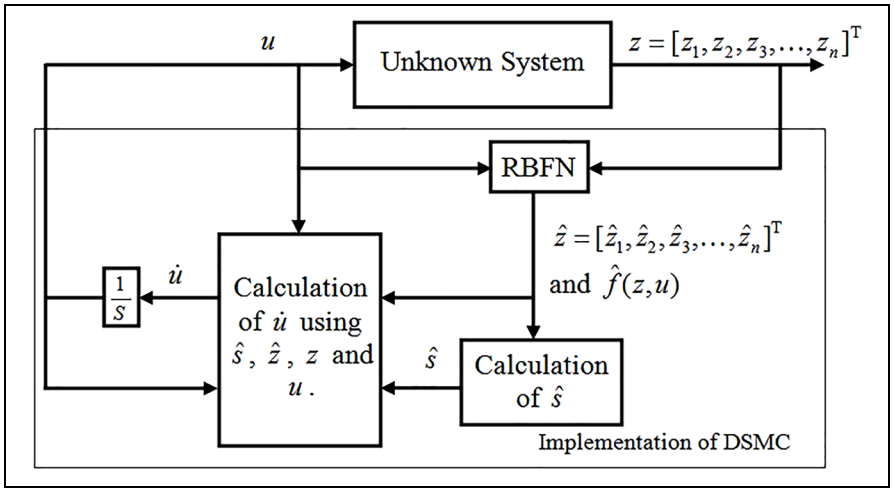

Figure 1. The proposed controller.
DSMC: dynamic sliding-mode control; RBFN: radial basis-function neural network.

Assume that $a_i: i = 1, 2, \ldots, n$ are such that A is stable, i.e., for any symmetric positive definite matrix Q, one can find a symmetric positive definite matrix P satisfying the Lyapunov equation, as

$$PA + A^{\mathrm{T}}P = -Q \tag{5}$$

Now, the objective is to utilize the DSMC to find an appropriate smooth input u such that the state vector $z(t) = [z_1(t), z_2(t), \cdots, z_n(t)]^{\mathrm{T}}$ tracks the desired trajectory. In DSMC, the integrator inserted before the input control law of the system filters the switching to obtain a smooth input u, with the result that chattering is suppressed. As mentioned in the introduction, for designing and applying DSMC to the system of equation (2), the function $g(z, u)$ should be estimated. The proposed approach is depicted in Figure 1; each block of this figure is explained in the following sections.

Neural observer for estimation of the plant model

According to the neural network theorems, RBFN can be approximated by any real continuous function with any arbitrary accuracy. In other words, the RBFN has a universal approximation property (Hovakimyan et al., 2002; Li, 2017; Lin and Hsu, 2004; Norgaard et al., 2000; Wang, 1997). Therefore, to estimate the nonlinear function g, a RBFN is used as follows

$$\begin{aligned} \dot{\hat{z}} &= A\hat{z} + B\hat{g} \\ \hat{g} &= \hat{w}^{\mathrm{T}}\xi(z, u) \end{aligned} \tag{6}$$

where $\hat{w} \in R^{m\times 1}$ is the estimate of the weight vector and $\xi(.): R^{n+1} \to R^{m\times 1}$ contains known Gaussian functions. Moreover $\hat{z} = [\hat{z}_1, \hat{z}_2, \hat{z}_3, \cdots, \hat{z}_n]^{\mathrm{T}}$ is the estimate of $z(t)$. Owing to the approximation capability of the RBFN, we have an ideal weight vector w with arbitrary large enough dimension m such that the system equation (2) can be written as

$$\begin{aligned} \dot{z} &= Az + Bg \\ g &= w^{\mathrm{T}}\xi(z, u) + \varepsilon \end{aligned} \tag{7}$$

where ε is an arbitrary small reconstruction error with bound B_ε, i.e., $|\varepsilon| < B_\varepsilon$ (Li, 2017). Now, the following estimator can be proposed

$$\dot{\hat{z}} = A\hat{z} + B\hat{w}^{\mathrm{T}}\xi(z, u) + k_z(z - \hat{z}) \tag{8}$$

where k_z is a positive number, which is determined in Theorem 1. By subtracting equation (8) from equation (7), one obtains

$$\dot{e}_z = Ae_z + Be_w^{\mathrm{T}}\xi(z, u) + B\varepsilon - k_z e_z \tag{9}$$

where $e_z = z - \hat{z}$ and $e_w = w - \hat{w}$ are the estimation errors of the state and parameter, respectively.

Theorem 1. *Using the following adaptive weight law*

$$\dot{\hat{w}} = k_w\xi(z, u)B^{\mathrm{T}}Pe_z - 4k_e k_w\|e_z\|\hat{w} \tag{10}$$

the estimation error $e_z(t)$ tends to zero if $k_z \to \infty$, where k_w and k_e are arbitrary positive scalar constants.

Proof. Assume the Lyapunov candidate function as follows

$$V(t) = \frac{1}{2}e_z^{\mathrm{T}}Pe_z + \frac{1}{2k_w}e_w^{\mathrm{T}}e_w \tag{11}$$

Then the time derivative of $V(t)$ would be

$$\dot{V}(t) = \frac{1}{2}\dot{e}_z^{\mathrm{T}}Pe_z + \frac{1}{2}e_z^{\mathrm{T}}P\dot{e}_z + \frac{1}{k_w}e_w^{\mathrm{T}}\dot{e}_w \tag{12}$$

Substituting equations (5) and (9) into equation (12), it follows that

$$\begin{aligned} \dot{V}(t) = &-\frac{1}{2}e_z^{\mathrm{T}}Qe_z + e_z^{\mathrm{T}}PB\varepsilon - k_z e_z^{\mathrm{T}}Pe_z \\ &+ e_w^{\mathrm{T}}\left(\frac{1}{k_w}\dot{e}_w + \xi(z, u)B^{\mathrm{T}}Pe_z\right) \end{aligned} \tag{13}$$

using $\dot{e}_w = -\dot{\hat{w}}$ and the tuning law (equation (10)) in equation (13) gives

$$\begin{aligned} \dot{V}(t) = &-\frac{1}{2}e_z^{\mathrm{T}}Qe_z + e_z^{\mathrm{T}}PB\varepsilon - k_z e_z^{\mathrm{T}}Pe_z \\ &+ 4k_e\|e_z\|e_w^{\mathrm{T}}\hat{w} \end{aligned} \tag{14}$$

Considering the properties of positive definite matrix Q and P, and using $\hat{w} = w - e_w$, this equation yields

$$\begin{aligned} \dot{V}(t) \leqslant &-\left(\frac{1}{2}\underline{\sigma}(Q) + k_z\underline{\sigma}(P)\right)\|e_z\|^2 \\ &+ \left(\overline{\sigma}(PB)B_\varepsilon - 4k_e(\|e_w\|^2 - B_w\|e_w\|)\right)\|e_z\| \end{aligned} \tag{15}$$

where $\overline{\sigma}$ and $\underline{\sigma}$ indicate the largest and smallest eigenvalues, respectively; moreover, $\|w\| < B_w$.

Now, B_{e_z} is defined as

$$B_{e_z} = \frac{\overline{\sigma}(PB)B_\varepsilon + k_e B_w^2}{\frac{1}{2}\underline{\sigma}(Q) + k_z\underline{\sigma}(P)} \tag{16}$$

Therefore

$$\begin{aligned} \dot{V}(t) \leqslant &-\left(\frac{1}{2}\underline{\sigma}(Q) + k_z\underline{\sigma}(P)\right)(\|e_z\| - B_{e_z})\|e_z\| \\ &- 4k_e\left(\|e_w\| - \frac{1}{2}B_w\right)^2\|e_z\| \end{aligned} \tag{17}$$

or

$$\dot{V}(t) \leqslant -\left(\frac{1}{2}\underline{\sigma}(Q) + k_z\underline{\sigma}(P)\right)(\|e_z\| - B_{e_z})\|e_z\| \tag{18}$$

Take

$$\omega(t) = \left(\frac{1}{2}\underline{\sigma}(Q) + k_z\underline{\sigma}(P)\right)(\|e_z\| - B_{e_z})\|e_z\|$$

and suppose $\|e_z\| > B_{e_z}$, then one can write $\dot{V} \leqslant -\omega(t) \leqslant 0$.

With integration over the interval $[0, t]$, we have

$$0 \leqslant \int_0^t \omega(\tau)\mathrm{d}\tau \leqslant \int_0^t \omega(\tau)\mathrm{d}\tau + V(t) \leqslant V(0) \tag{19}$$

When $t \to \infty$, the integral equation (19) exists and would be less than or equal to $V(0)$. Since $V(0)$ is finite with positive value, then based on Barbalat's lemma (Slotine and Li, 1991), we have

$$\begin{aligned}\lim_{t\to\infty}\omega(t) &= \lim_{t\to\infty}\left(\frac{1}{2}\underline{\sigma}(Q) + k_z\underline{\sigma}(P)\right)(\|e_z\| - B_{e_z})\|e_z\| \\ &= 0\end{aligned} \tag{20}$$

Since

$$\left(\frac{1}{2}\underline{\sigma}(Q) + k_z\underline{\sigma}(P)\right)$$

is greater than zero, equation (20) implies decreasing $\|e_z\|$ until it becomes less than B_{e_z} with the result that $\lim_{t\to\infty}\|e_z\| \leqslant B_{e_z}$. This guarantees that B_{e_z} is the upper bound of $\|e_z\|$ and it is clear that $\lim_{k_z\to\infty} B_{e_z} = 0$. Then the bound of $\|e_z\|$ or e_z will converge to zero if $k_z \to \infty$.

Designing the proposed dynamic sliding-mode controller (DSMC)

The surface in conventional sliding-mode control can be defined as (Perruquetti and Barbot, 2002; Slotine and Li, 1991; Young et al., 1996)

$$s(t) = \left(\lambda + \frac{\mathrm{d}}{\mathrm{d}t}\right)^{n-1} e(t) \tag{21}$$

where $e(t) = z_1(t) - r(t)$ and $r(t)$ is a reference. To implement DSMC and incorporate the Jacobean of the neural dynamic model of the plant as an approximation of the Jacobean of the plant, we include the nth-order derivative term to the sliding surface and use the error of model output with respect to desired reference instead. Thus, the following sliding surface would be considered, which is used in DSMC (Chen et al., 2007; Karami-Mollaee et al., 2011)

$$s(t) = \left(\lambda + \frac{\mathrm{d}}{\mathrm{d}t}\right)^{n} \hat{e}(t) \tag{22}$$

where $\hat{e}(t) = \hat{z}_1(t) - r(t)$, $\hat{z}_1(t)$ denotes the estimate of $z_1(t)$ and also $\lambda > 0$ represents a scalar constant. The DSMC sliding surface (equation (22)) can be described as

$$s(t) = \sum_{j=0}^{n}\binom{n}{j}\lambda^{n-j}\hat{z}_1^{(j)}(t) - \sum_{j=0}^{n}\binom{n}{j}\lambda^{n-j}r^{(j)}(t) \tag{23}$$

Lemma 1. *The following two equalities hold*

$$\begin{aligned}\hat{z}_1^{(m)} &= \hat{z}_{m+1} \\ &+ \sum_{i=1}^{m}\left\{(-1)^{m-i}\binom{m}{i-1}k_z^{m-i+1},(z_i - \hat{z}_i)\right\}\end{aligned} \tag{24}$$

where $m = 1, \ldots, n-1$, *and*

$$\begin{aligned}\hat{z}_1^{(n)} &= \sum_{i=1}^{n} -a_{n-i+1}\hat{z}_i \\ &+ \sum_{i=1}^{n}\left\{(-1)^{n-i}\binom{n}{i-1}k_z^{n-i+1}(z_i - \hat{z}_i)\right\} \\ &+ \hat{w}^{\mathrm{T}}\xi(z,u)\end{aligned} \tag{25}$$

Proof. The proof is given in the appendix.

Substituting equations (24) and (25) into equation (23) yields

$$s(t) = d(t) + \hat{w}^{\mathrm{T}}\xi(z,u) + nk_z z_n \tag{26}$$

where

$$\begin{aligned}d(t) &= \sum_{j=0}^{n-1}\binom{n}{j}\lambda^{n-j}\hat{z}_1^{(j)}(t) + \sum_{i=1}^{n} -a_{n-i+1}\hat{z}_i \\ &+ \sum_{i=1}^{n-1}\left\{(-1)^{n-i}\binom{n}{i-1}k_z^{n-i+1}(z_i - \hat{z}_i)\right\} \\ &- \sum_{j=0}^{n}\binom{n}{j}\lambda^{n-j}r^{(j)}(t) - nk_z\hat{z}_n\end{aligned} \tag{27}$$

Taking the derivative of equation (26), one has

$$\dot{s}(t) = h + \hat{w}^{\mathrm{T}}\frac{\partial\xi(z,u)}{\partial z_n}\dot{z}_n + \hat{w}^{\mathrm{T}}\frac{\partial\xi(z,u)}{\partial u}\dot{u} + nk_z\dot{z}_n \tag{28}$$

where

$$h(t) = \dot{d}(t) + \dot{\hat{w}}^{\mathrm{T}}\xi(z,u) + \hat{w}^{\mathrm{T}}\sum_{i=1}^{n-1}\frac{\partial\xi(z,u)}{\partial z_i}\dot{z}_i \tag{29}$$

Note that the function $h(t)$ can be denoted $h(z,\hat{z},\hat{w},\xi,\partial\xi/\partial z)$ which means that $h(t)$ is a known function. This can be shown by substituting equations (10), (24), (25), (42) and (43) into equation (29) and the derivative of equation (27). The following theorem offers a stabilizing control law based on this sliding surface.

Theorem 2. *For the system given in equation (2) and its neural model given in equation (8), let the adaptive controller be*

$$\begin{aligned}\dot{u}(t) &= \left(\hat{w}^{\mathrm{T}}\frac{\partial\xi(z,u)}{\partial u}\right)^{-1} \\ &\times\left[-\left|\hat{w}^{\mathrm{T}}\frac{\partial\xi(z,u)}{\partial z_n} + nk_z\right|\rho(z,u)\mathrm{sign}(s) - h\right]\end{aligned} \tag{30}$$

whereas

$$|f(z,u)| < \rho(z,u) \tag{31}$$

and ρ *is the known upper bound of* $|f|$. *The function* ρ *can be a constant or a function of* z *and* u, *generally depending on a-priori knowledge about the extreme behaviour of the unknown plant. Then the nonlinear controller defined in equation (30) leads the state variables of the system to the sliding surface*

(equation (22)) in finite time and drives an arbitrary initial value of $s(t)$ to zero.

Proof. Assume a Lyapunov candidate function of the form $V(t) = 0.5s(t)^2$. Then, one has $\dot{V}(t) = s(t)\dot{s}(t)$. Using equation (28), we have

$$\dot{V}(t) = s(t)\left[h + \hat{w}^{\mathrm{T}}\frac{\partial \xi(z,u)}{\partial z_n}f(z,u) + \hat{w}^{\mathrm{T}}\frac{\partial \xi(z,u)}{\partial u}\dot{u} + nk_z f(z,u)\right] \tag{32}$$

Substituting equation (30) into this equation yields

$$\dot{V}(t) = -\left|\hat{w}^{\mathrm{T}}\frac{\partial \xi(z,u)}{\partial z_n} + nk_z\right||s(t)|\rho(z,u) + \left(\hat{w}^{\mathrm{T}}\frac{\partial \xi(z,u)}{\partial z_n} + nk_z\right)f(z,u)s(t) \tag{33}$$

This yields

$$\dot{V}(t) \leqslant -\left|\hat{w}^{\mathrm{T}}\frac{\partial \xi(z,u)}{\partial z_n} + nk_z\right||s(t)|\rho(z,u) + \left|\hat{w}^{\mathrm{T}}\frac{\partial \xi(z,u)}{\partial z_n} + nk_z\right||f(z,u)||s(t)| \tag{34}$$

Then one can write equation (34) as

$$\dot{V}(t) \leqslant \left|\hat{w}^{\mathrm{T}}\frac{\partial \xi(z,u)}{\partial z_n} + nk_z\right||s(t)|(|f(z,u)| - \rho(z,u)) < 0 \tag{35}$$

Numerical simulations

In this section, two numerical examples are carried out by applying two different nonlinear non-affine systems to validate the effectiveness of these proposed methods. Both simulations are conducted using Matlab with a sampling time of 0.001s.

Example 1

Consider the following Duffing–Holmes chaotic system (Li et al., 2010)

$$\begin{aligned} \dot{z}_1 &= z_2 \\ \dot{z}_2 &= f(z,u) \\ f(z,t) &= b_1 z_1 + b_2 z_2 + b_3 {z_1}^3 + b_4 \cos(1.2t) + u \\ z &= [z_1, z_2]^{\mathrm{T}} \end{aligned} \tag{36}$$

where b_2 is the damping ratio, $b_1 z_1 + b_3 z_1^3$ is a recoverability term, $b_4 \cos(1.2t)$ represents the force period and u is set as the input control signal. To ensure that the system has chaotic behaviour, the constant parameters are chosen as $b_1 = 1.0, b_2 = -0.20, b_3 = -1.0$ and $b_4 = 0.32$, with the initial condition $z(0) = [z_1(0), z_2(0)]^{\mathrm{T}} = [1, 2]^{\mathrm{T}}$. Note that in chaos systems, states are bounded and then equation (31) holds, as shown in Figure 2. As can be seen, the chaotic behaviour of the system and the boundedness of its model are clear, such that $|f(z,t)| \leqslant 6$ and then $\rho = 6$. We choose an RBFN with three inputs (z_1, z_2, u), nine radial basis-function neurons in the hidden layer and one output $\hat{g}$. The neural network tuning parameters have been chosen as $k_w = 2, k_z = 50$ and $k_e = 0.1$. Other parameters are chosen as $\lambda = 7$ and

$$P = \begin{bmatrix} 15 & 5 \\ 5 & 5 \end{bmatrix}, \qquad A = \begin{bmatrix} 0 & 1 \\ -200 & -100 \end{bmatrix} \tag{37}$$

The initial conditions for the neural network are $w(0) = [0, 0, \cdots, 0]^{\mathrm{T}}$. Note that the initial conditions for the neural network can be chosen arbitrarily. The objective is to force $z_1(t)$ to follow the output $r(t)$ of the system $\ddot{r} = -5r - 3\dot{r} + u_{\mathrm{d}}$ as a desired reference, where, u_{d} is $\sin(t)$, i.e., $u_{\mathrm{d}} = \sin(t)$, which is shown in Figure 6(b). The other results are shown in Figures 3, 4, 5, 6 and 7.

Figures 3 and 4 show the capability of the proposed RBFN to produce first and second estimates of the system. Moreover, as is apparent from these figures, the reference trajectory is tracked. Figure 5(a) demonstrates the simulation result of the neural network to approximate the unknown nonlinear functions. As can be seen, the output of RBFN

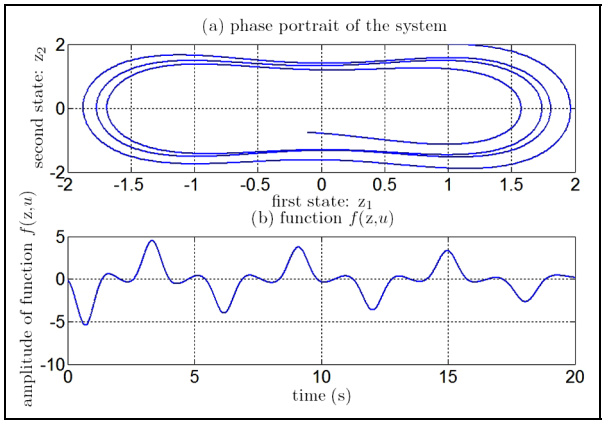

Figure 2. (a) The chaotic behaviour of the system. (b) The bounded nonlinear system.

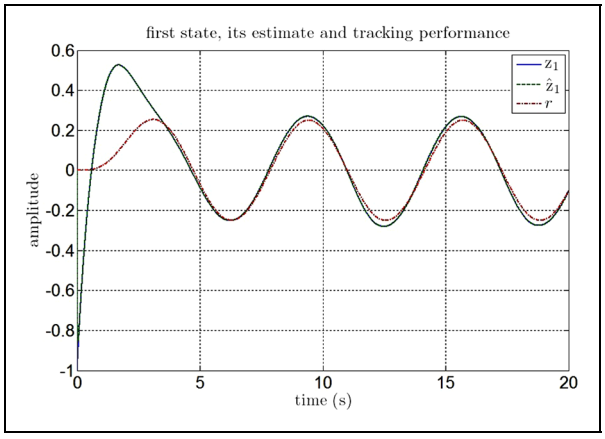

Figure 3. Tracking performance of first state in Duffing–Holmes chaotic system.

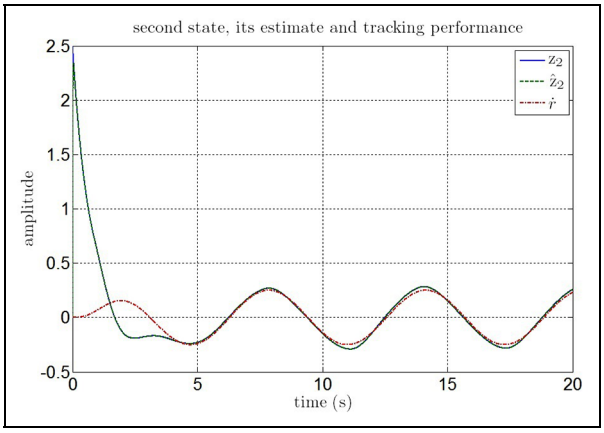

Figure 4. Tracking performance of second state in Duffing–Holmes chaotic system.

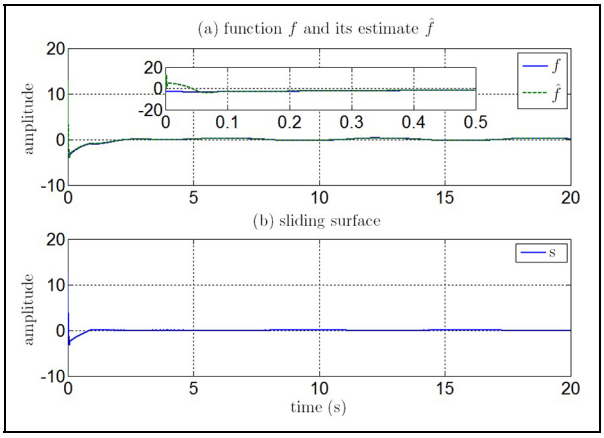

Figure 5. (a) Duffing–Holmes chaotic system estimation model. (b) Convergence of sliding surface to zero in finite time.

follows the output of nonlinear function. From Figure 5(b), we can see that the convergence to the sliding surface occurs in finite time. The input control signal of the nonlinear Duffing–Holmes chaotic system is shown in Figure 6(a), which is smooth and does not show any switching. The estimation convergence of the proposed neural network weight vector is included in Figure 7 to show the performance of the proposed method.

Example 2

Assume the one-phase model of a switch reluctance motor (Xu and Tan, 2002), as

$$\begin{aligned}\dot{z}_1 &= z_2\\ \dot{z}_2 &= f(z,u,t)\\ &= \frac{N_r^2\psi_s}{Jh^2(z_1)}\frac{\mathrm{d}h(z_1)}{\mathrm{d}z_1}\\ &\quad\times\{1-[1+uh(z_1)]\exp(-uh(z_1))\}-\frac{T}{J}\end{aligned}$$

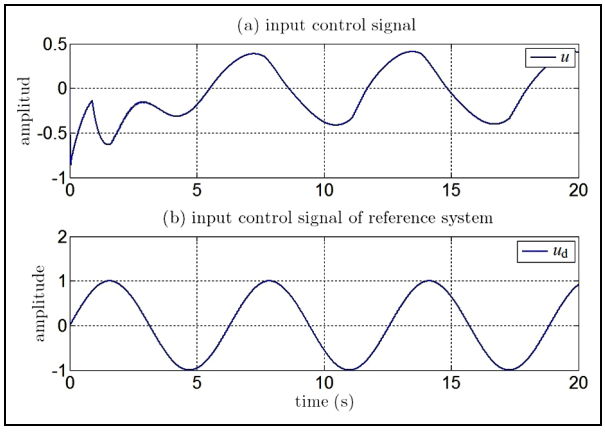

Figure 6. (a) Input control signal of Duffing–Holmes chaotic system. (b) Input control signal of reference system.

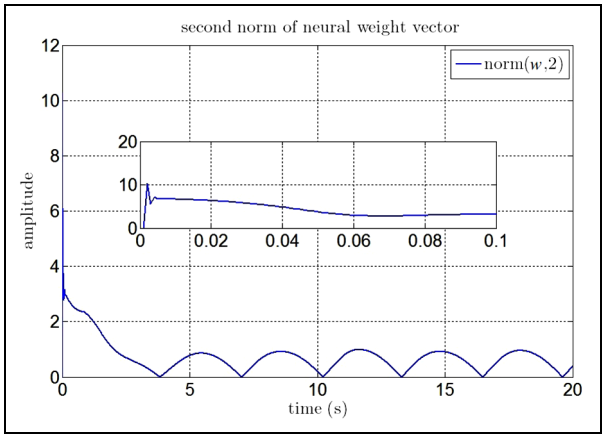

Figure 7. Convergence of second norm of neural network weight vectors for Duffing–Holmes chaotic system.

$$\begin{aligned}h(z_1) &= L_a + L_u\sin(z_1)\\ z &= [z_1, z_2]^T\end{aligned} \tag{38}$$

Where z_1 and z_2 represent the electrical angular position, and the mechanical angular velocity, respectively. u denotes the input control (stator current) signal, N_r gives the number of rotor poles, ψ_s is the flux linkage, J is the total rotor of load inertia, T is the load torque and L_a and L_u are the value of inductance at the aligned and un-aligned positions, respectively. In this example, the switch reluctance motor parameters are chosen as $N_r = 4.0$, $J = 0.07$ kg.m^2, $\psi_s = 0.1$ Wb, $L_a = 180$ mH, $L_u = 8$ mH and $T = 0.5$ N.M. Consider that the uncertainty is only in L_a and L_u. In addition, suppose that one knows

$$5\text{ mH} \leqslant L_u \leqslant 15\text{ mH}, \qquad 170\text{ mH} \leqslant L_a \leqslant 210\text{ mH} \tag{39}$$

Lemma 2. *Assume that the switch reluctance motor with the uncertainties is*

$$0 < \alpha \leqslant L_u \leqslant \beta < \gamma \leqslant L_a \leqslant \delta \tag{40}$$

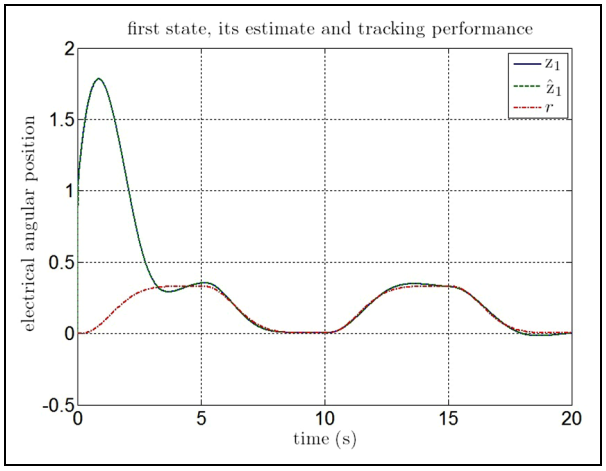

Figure 8. Tracking performance of first state in switch reluctance motor.

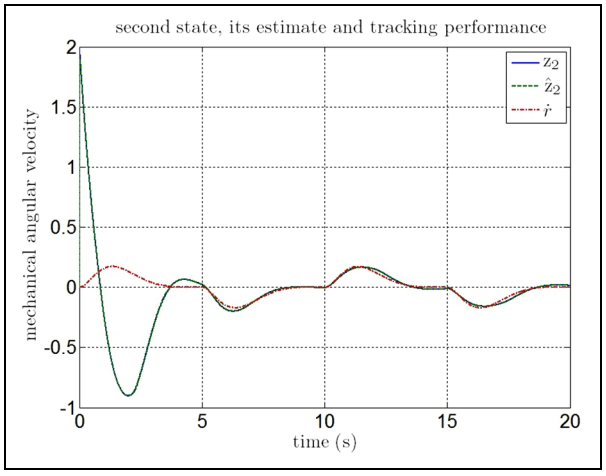

Figure 9. Tracking performance of second state in switch reluctance motor.

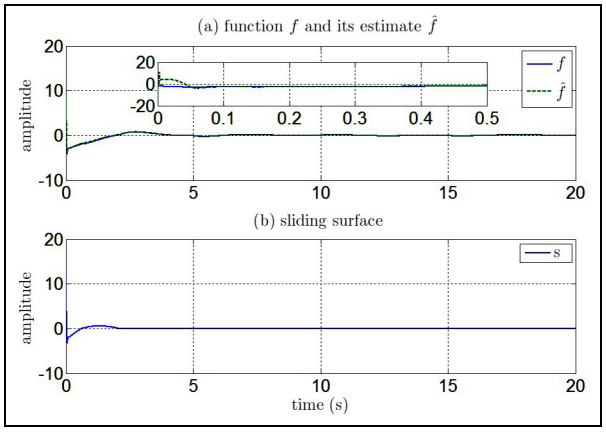

Figure 10. (a) Switch reluctance motor estimation model. (b) Convergence of sliding surface to zero in finite time.

Then, one has

$$|f - \hat{f}| \leqslant \Delta_f \tag{41}$$

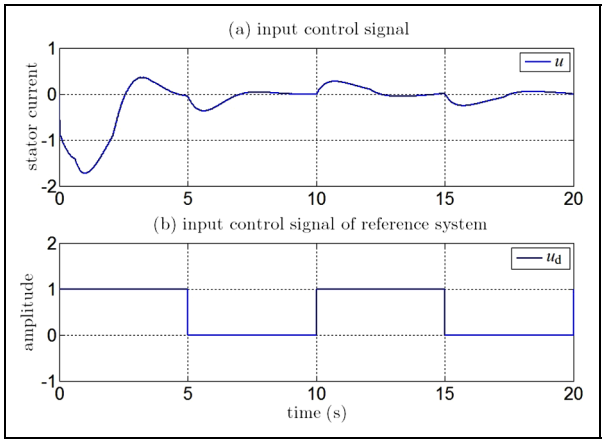

Figure 11. (a) Input control signal of switch reluctance motor. (b) Input control signal of reference system.

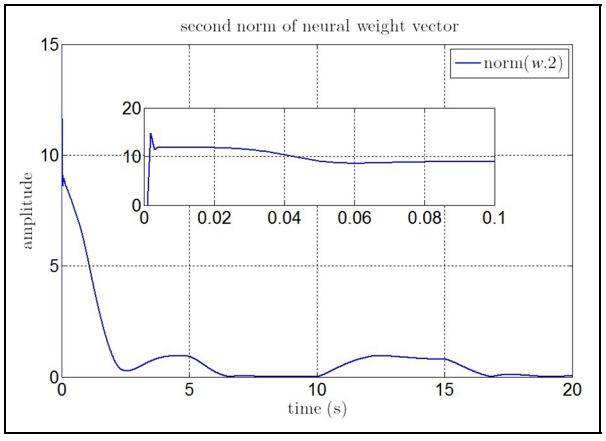

Figure 12. Convergence of second norm of neural network weight vectors for switch reluctance motor.

where

$$\Delta_f = \frac{2N_r^2\psi_s}{J}\left[\frac{\beta + \beta(1 + (\delta + \beta)|u|)\exp(-(\gamma - \beta)|u|)}{(\gamma - \beta)^2}\right]$$

Proof. The proof is given in the appendix.

Then we have $|f| \leqslant |\hat{f}| + \Delta_f$; in order to have $|f| < \rho$, we choose $\rho = |\hat{f}| + \Delta_f + 0.1$ and select $\hat{L}_a = 170$ mH, $\hat{L}_u = 10$ mH and consider that the system state variables are initially chosen as $z(0) = [z_1(0), z_2(0)]^T = [1, 2]^T$. All the other parameters are as in the previous example. The objective is to force $z_1(t)$ to follow the output $r(t)$ of the system $\ddot{r} = -5r - 3\dot{r} + u_d$ as a desired reference, where u_d is a periodic step signal, which is shown in Figure 11(b). Other results are shown in Figures 8, 9, 10 and 11. The estimation convergence of the proposed neural network weight vector is included in Figure 12, to show the performance of the proposed method.

The results of these two simulations illustrate good transient performance; the tracking error is small with all signals in the closed loop system being bounded.

Conclusion

In this study, a robust adaptive DSMC is developed for tracking control of a dynamic, non-affine, nonlinear, unknown system using RBFNs. By using a robust adaptation law, a model is obtained for the unknown nonlinear function of the plant. By adding the *n*th-order derivative term of the error to the sliding surface, it is possible to incorporate the approximate information of the plant (i.e., the plant neural model) in deriving the nonlinear adaptive controller. Moreover, the tracking error vector was driven to the sliding manifold with a smooth control effort. This method does not require any off-line training phase for the neural network. The developed control structure has fast convergence and removes the chattering problem without degrading the tracking performance. To verify the effectiveness of the approach, two nonlinear examples are given; a Duffing–Holmes chaotic system and a switch reluctance motor.

Declaration of conflicting interests

The author(s) declared no potential conflicts of interest with respect to the research, authorship, and/or publication of this article.

Funding

The author(s) received no financial support for the research, authorship, and/or publication of this article.

References

Amer AF, Sallam EA and Elawady WM (2011) Adaptive fuzzy sliding mode control using supervisory fuzzy control for 3 DOF planar robot manipulators. *Applied Soft Computing* 11(8): 4943–4953.

Bartolini G, Ferrara A and Usai E (1998) Chattering avoidance by second-order sliding mode control. *IEEE Transactions on Automatic Control* 43(2): 241–246.

Boiko I, Fridman L and Iriarte R (2005) Analysis of chattering in continuous sliding mode control. In: *American control conference*, Portland, OR, USA, 8–10 June 2005, pp. 2439–2444. Piscataway, NJ: IEEE.

Bouzeriba A, Boulkroune A and Bouden T (2016) Projective synchronization of two different fractional-order chaotic systems via adaptive fuzzy control. *Neural Computing and Applications* 27(5): 1349–1360.

Cavallo A and Natale C (2003) Output feedback control based on a high-order sliding manifold approach. *IEEE Transactions on Automatic Control* 48(3): 469–472.

Chen MS, Chen CH and Yang FY (2007) An LTR-observer-based dynamic sliding mode control for chattering reduction. *Automatica* 43(6): 1111–1116.

Chen MS, Hwang YR and Tomizuka M (2002) A state-dependent boundary layer design for sliding mode control. *IEEE Transactions on Automatic Control* 47(10): 1677–1681.

Erbatur K and Kaynak O (2001) Use of adaptive fuzzy systems in parameter tuning of sliding-mode controllers. *IEEE/ASME Transactions on Mechatronics* 6(4): 474–482.

Hao Z, Xing-Yuan W and Xiao-Hui L (2016) Synchronization of complex-valued neural network with sliding mode control. *Journal of the Franklin Institute* 353(2): 345–358.

Hovakimyan N, Nardi F and Calise AJ (2002) A novel error observer-based adaptive output feedback approach for control of uncertain systems. *IEEE Transactions on Automatic Control* 47(8): 1310–1314.

Karami-Mollaee A, Pariz N and Shanechi H (2011) Position control of servomotors using neural dynamic sliding mode. *Journal of Dynamic Systems, Measurement, and Control* 133(6): 061014.

Kaynak O, Erbatur K and Ertugnrl M (2001) The fusion of computationally intelligent methodologies and sliding-mode control – a survey. *IEEE Transactions on Industrial Electronics* 48(1): 4–17.

Laghrouche S, Plestan F and Glumineau A (2007) Higher order sliding mode control based on integral sliding mode. *Automatica* 43(3): 531–537.

Lee H and Utkin VI (2007) Chattering suppression methods in sliding mode control systems. *Annual Reviews in Control* 31(2): 179–188.

Levant A (1993) Sliding order and sliding accuracy in sliding mode control. *International Journal of Control* 58(6): 1247–1263.

Levant A (1998) Robust exact differentiation via sliding mode technique. *Automatica* 34(3): 379–384.

Levant A (2003) Higher-order sliding modes, differentiation and output-feedback control. *International Journal of Control* 76(9–10): 924–941.

Levant A (2005) Homogeneity approach to high-order sliding mode design. *Automatica* 41(5): 823–830.

Li C (2017) Innovation of film and television directoring mode based on big data mining platform. *Boletn Técnico* 55(16): 149–155.

Li W, Lan T and Lin W (2010) Adaptive tracking control of Duffing–Holmes chaotic systems with uncertainty. In: *5th international conference on computer science and education (ICCSE)*, Hefei, China, 24–27 August 2010, pp. 1193–1197. Piscataway, NJ: IEEE.

Lin CM and Hsu CF (2004) Adaptive fuzzy sliding-mode control for induction servomotor systems. *IEEE Transactions on Energy Conversion* 19(2): 362–368.

Moghaddam JJ, Farahani MH and Amanifard N (2011) A neural network-based sliding-mode control for rotating stall and surge in axial compressors. *Applied Soft Computing* 11(1): 1036–1043.

Norgaard M, Ravn O, Poulsen N, et al. (2000) *Neural Networks for Modelling and Control of Dynamic Systems: A Practitioner's Handbook*. Berlin: Springer.

Perruquetti W and Barbot JP (2002) *Sliding Mode Control in Engineering*. Boca Raton, FL: CRC Press.

Slotine JJE and Li W (1991) *Applied Nonlinear Control*. Englewood Cliffs, NJ: Prentice Hall.

Sun T, Pei H, Pan Y, et al. (2011) Neural network-based sliding mode adaptive control for robot manipulators. *Neurocomputing* 74(14–15): 2377–2384.

Wang L (1997) *A Course in Fuzzy Systems and Control*. Upper Saddle River, NJ: Prentice-Hall.

Wong LK, Leung FHF and Tam PKS (2001) A fuzzy sliding controller for nonlinear systems. *IEEE Transactions on Industrial Electronics* 48(1): 32–37.

Wu H, Wang L, Niu P, et al. (2017) Global projective synchronization in finite time of nonidentical fractional-order neural networks based on sliding mode control strategy. *Neurocomputing* 235: 264–273.

Xu G, Liu F, Xiu C, et al. (2016) Optimization of hysteretic chaotic neural network based on fuzzy sliding mode control. *Neurocomputing* 189: 72–79.

Xu JX and Tan Y (2002) On the P-type and Newton-type ILC schemes for dynamic systems with non-affine-in-input factors. *Automatica* 38(7): 1237–1242.

Yang Y and Yan Y (2016) Neural network approximation-based nonsingular terminal sliding mode control for trajectory tracking of robotic airships. *Aerospace Science and Technology* 54: 192–197.

Yildiz Y, Sabanovic A and Abidi K (2007) Sliding-mode neurocontroller for uncertain systems. *IEEE Transactions on Industrial Electronics* 54(3): 1676–1685.

Young KD, Utkin VI and Ozguner U (1996) A control engineer's guide to sliding mode control. In: *International workshop on variable structure systems*, Tokyo, Japan, 5–6 December. Piscataway, NJ: IEEE.

Appendix

Proof of Lemma 1

We prove equations (24) and (25) by induction. Using equation (8), we obtain

$$\dot{\hat{z}}_i = \hat{z}_{i+1} + k_z(z_i - \hat{z}_i):\ i = 1, 2, \ldots, n-1 \tag{42}$$

$$\dot{\hat{z}}_n = \sum_{i=1}^{n} -a_{n-i+1}\hat{z}_i + k_z(z_n - \hat{z}_n) + \hat{w}^{\mathrm{T}}\xi(z,u) \tag{43}$$

For $m = 1$, equation (24) reduces to equation (42), where $i = 1$. Now assume that equation (24) holds for some $m < n-1$; we prove that it also holds for $m+1$, i.e.

$$\hat{z}_1^{(m+1)} = \hat{z}_{m+2} + \sum_{i=1}^{m+1}\left\{(-1)^{m+1-i}\binom{m+1}{i-1}k_z^{m-i+2}(z_i - \hat{z}_i)\right\} \tag{44}$$

To prove this, we take the derivative of equation (24), which yields

$$\hat{z}_1^{(m+1)} = \dot{\hat{z}}_{m+1} + \sum_{i=1}^{m}\left\{(-1)^{m-i}\binom{m}{i-1}k_z^{m-i+1}(\dot{z}_i - \dot{\hat{z}}_i)\right\} \tag{45}$$

Using equation (42), we can write this equation as

$$\hat{z}_1^{(m+1)} = \hat{z}_{m+2} + k_z(z_{m+1} - \hat{z}_{m+1}) + \sum_{i=1}^{m}\left\{(-1)^{m-i}\binom{m}{i-1}k_z^{m-i+1}\Big(z_{i+1} - \hat{z}_{i+1} - k_z(z_i - \hat{z}_i)\Big)\right\} \tag{46}$$

or

$$\begin{aligned}\hat{z}_1^{(m+1)} = {} & \hat{z}_{m+2} + k_z(m+1)(z_{m+1} - \hat{z}_{m+1}) \\ & + \sum_{i=1}^{m-1}\left\{(-1)^{m-i}\binom{m}{i-1}k_z^{m-i+1}(z_{i+1} - \hat{z}_{i+1})\right\} \\ & + \sum_{i=2}^{m}\left\{(-1)^{m-i+1}\binom{m}{i-1}k_z^{m-i+2}(z_i - \hat{z}_i)\right\} \\ & + (-1)^m k_z^{m+1}(z_1 - \hat{z}_1)\end{aligned} \tag{47}$$

Changing $i \to i-1$ in the second term of the right side of equation (47) and then using the identity

$$\binom{m}{i-2} + \binom{m}{i-1} = \binom{m+1}{i-1}$$

we have

$$\begin{aligned}\hat{z}_1^{(m+1)} = {} & \hat{z}_{m+2} + (-1)^m k_z^{m+1}(z_1 - \hat{z}_1) \\ & + k_z(m+1)(z_{m+1} - \hat{z}_{m+1}) \\ & + \sum_{i=2}^{m}\left\{(-1)^{m+1-i}\binom{m+1}{i-1}k_z^{m-i+2}(z_i - \hat{z}_i)\right\}\end{aligned} \tag{48}$$

This equation can be simplified as equation (44). This proves the validity of equation (24). Moreover, equation (25) is easily proven by setting $m = n-1$ in equation (45), substituting $\dot{\hat{z}}_n$ in equation (43) (instead of equation (42)) and following derivations similar to equation (46) up to equation (48). The proof is completed.

Proof of Lemma 2

The switch reluctance motor system model can be represented in the following form with $T = 0$

$$\begin{aligned}\ddot{z} &= f(z,u,t) \\ &= \frac{{N_{\mathrm{r}}}^2\psi_{\mathrm{s}}}{J}\left\{\frac{1}{h^2}\frac{\mathrm{d}h}{\mathrm{d}z} - \frac{1}{h^2}\frac{\mathrm{d}h}{\mathrm{d}z}(1+uh)\exp(-uh)\right\} \\ h(z) &= L_{\mathrm{a}} + L_{\mathrm{u}}\sin(z)\end{aligned} \tag{49}$$

Thus, we have the following inequalities

$$-\beta \leqslant L_{\mathrm{u}}\sin(z) \leqslant +\beta \tag{50}$$

$$\gamma - \beta \leqslant h \leqslant \delta + \beta \tag{51}$$

$$-\beta \leqslant \frac{\mathrm{d}h}{\mathrm{d}z} \leqslant +\beta \tag{52}$$

$$\frac{1}{(\delta+\beta)^2} \leqslant \frac{1}{h^2} \leqslant \frac{1}{(\gamma-\beta)^2} \tag{53}$$

$$\frac{-\beta}{(\gamma-\beta)^2} \leqslant \frac{1}{h^2}\frac{\mathrm{d}h}{\mathrm{d}z} \leqslant \frac{+\beta}{(\gamma-\beta)^2} \tag{54}$$

Consider $u < 0$. Then

$$(\delta+\beta)u \leqslant uh \leqslant (\gamma-\beta)u \tag{55}$$

$$-(\gamma-\beta)u \leqslant -uh \leqslant -(\delta+\beta)u \tag{56}$$

$$\exp(-(\gamma-\beta)u) \leqslant \exp(-uh) \leqslant \exp(-(\delta+\beta)u) \tag{57}$$

$$1 + (\delta+\beta)u \leqslant 1 + uh \leqslant 1 + (\gamma-\beta)u \tag{58}$$

Now, let us consider three cases as follows.

Case I. Assume that

$$1 + (\delta+\beta)u > 0, \qquad 1 + (\gamma-\beta)u > 0 \tag{59}$$

Then

$$\begin{aligned}&[1 + (\delta+\beta)u]\exp(-(\gamma-\beta)u) \\ &\quad \leqslant (1+uh)\exp(-uh) \\ &\quad \leqslant [1 + (\gamma-\beta)u]\exp(-(\delta+\beta)u)\end{aligned} \tag{60}$$

$$
\begin{aligned}
&-\frac{\beta[1+(\gamma-\beta)u]\exp(-(\delta+\beta)u)}{(\gamma-\beta)^2}\\
&\quad\leqslant \frac{1}{h^2}\frac{\mathrm{d}h}{\mathrm{d}z}(1+uh)\exp(-uh) \qquad (61)\\
&\quad\leqslant +\frac{\beta[1+(\gamma-\beta)u]\exp(-(\delta+\beta)u)}{(\gamma-\beta)^2}\\
&-\frac{\beta+\beta[1+(\gamma-\beta)u]\exp(-(\delta+\beta)u)}{(\gamma-\beta)^2}\\
&\quad\leqslant \frac{1}{h^2}\frac{\mathrm{d}h}{\mathrm{d}z}-\frac{1}{h^2}\frac{\mathrm{d}h}{\mathrm{d}z}(1+uh)\exp(-uh) \qquad (62)\\
&\quad\leqslant +\frac{\beta+\beta[1+(\gamma-\beta)u]\exp(-(\delta+\beta)u)}{(\gamma-\beta)^2}
\end{aligned}
$$

and finally

$$
\begin{aligned}
&|f-\hat{f}|\\
&\leqslant \frac{2N_{\mathrm{r}}{}^2\psi_{\mathrm{s}}}{J}\left[\frac{\beta+\beta(1+(\gamma-\beta)|u|)\exp(-(\delta+\beta)|u|)}{(\gamma-\beta)^2}\right] \qquad (63)
\end{aligned}
$$

Case II. Assume that

$$1+(\delta+\beta)u<0, \qquad 1+(\gamma-\beta)u<0 \qquad (64)$$

Then

$$
\begin{aligned}
&|f-\hat{f}|\\
&\leqslant \frac{2N_{\mathrm{r}}{}^2\psi_{\mathrm{s}}}{J}\left[\frac{\beta+\beta(1+(\delta+\beta)|u|)\exp(-(\delta+\beta)|u|)}{(\gamma-\beta)^2}\right] \qquad (65)
\end{aligned}
$$

Case III. Assume that

$$1+(\delta+\beta)u<0, \qquad 1+(\gamma-\beta)u>0 \qquad (66)$$

Then

$$
\begin{aligned}
&|f-\hat{f}|\leqslant\\
&\frac{2N_{\mathrm{r}}{}^2\psi_{\mathrm{s}}}{J}\left[\frac{\beta+\beta(1+(\gamma-\beta)|u|)\exp(-(\delta+\beta)|u|)}{(\gamma-\beta)^2}\right] \qquad (67)
\end{aligned}
$$

or

$$
\begin{aligned}
&|f-\hat{f}|\\
&\leqslant \frac{2N_{\mathrm{r}}{}^2\psi_{\mathrm{s}}}{J}\left[\frac{\beta+\beta(1+(\delta+\beta)|u|)\exp(-(\delta+\beta)|u|)}{(\gamma-\beta)^2}\right] \qquad (68)
\end{aligned}
$$

Now suppose $u>0$. Then

$$
\begin{aligned}
&|f-\hat{f}|\\
&\leqslant \frac{2N_{\mathrm{r}}{}^2\psi_{\mathrm{s}}}{J}\left[\frac{\beta+\beta(1+(\delta+\beta)|u|)\exp(-(\gamma-\beta)|u|)}{(\gamma-\beta)^2}\right] \qquad (69)
\end{aligned}
$$

It is clear that

$$\delta+\beta>\gamma-\beta \qquad (70)$$

Thus, one can infer equation (41) from equations (63), (65), (67), (68), (69) and (70).